Energy levels of a hydrogenic impurity in GaAs/$Ga_{1-x}Al_xAs$ multiple-quantum-well structures with narrow barriers in a magnetic field

N. Nguyen, J. X. Zang, R. Ranganathan, B. D. McCombe, and M. L. Rustgi
Department of Physics and Astronomy, State University of New York at Buffalo, Buffalo, New York 14260
(Received 21 June 1993)

A variational approach employing Gaussian-type trial wave functions and mixing of miniband states has been used to calculate the binding energies of the ground and first excited states of a hydrogenic donor in multiple-quantum-well structures consisting of a varying number of GaAs quantum wells separated by thin $Ga_{1-x}Al_xAs$ barriers with periodicities of 89 Å (80-Å well and 9-Å barrier) and 49 Å (40-Å well and 9-Å barrier). The dependence of the binding energies on two different positions (on center and on edge of the central well) was investigated. It was found that the binding energies did not change in any significant way beyond 15 periods for either of the structures investigated at zero magnetic field. Calculations were also performed for superlattice structures with 15 periods in the presence of a magnetic field applied perpendicular to the interfaces. Results have been compared with recent experimental measurements for donor transition energies in $GaAs/Ga_{0.7}Al_{0.3}As$ superlattices. Very good agreement is obtained.

I. INTRODUCTION

The developments of modern semiconductor crystal growth techniques, such as molecular-beam epitaxy and metal-organic chemical vapor deposition, have made possible the realization of high-quality superlattice and multiple-quantum-well structures of many functional forms of the confining wells and barriers. These, in turn, have found applications in a variety of new devices and led to the development of the ultrahigh-speed resonant tunneling diode.[1–7]

The problem of shallow impurities in $GaAs/Ga_{1-x}Al_xAs$ quantum wells and superlattices has been a key problem and has attracted a great deal of attention in the past few years. The problem in a quantum well with infinite barrier height was first treated theoretically by Bastard.[8] Mailhiot, Chang, and McGill[9] and Green and Bajaj[10] independently calculated the energies of the ground state and few excited states of a hydrogenic impurity in the $GaAs/Ga_{1-x}Al_xAs$ quantum well using a variational method. These studies were a significant improvement over the earlier calculations of Bastard, which departed somewhat from the realistic situation. The effect of image forces due to the difference in static dielectric constants in the GaAs and $Ga_{1-x}Al_xAs$ on the energy spectrum of the donor impurity in the quantum well was also studied by Mailhiot, Chang, and McGill.[9] The calculations of Green and Bajaj for the $1s$-$2p_-$ and $1s$-$2p_+$ transitions were found to be in good agreement with the observations of Jarosik *et al.*[11] Chaudhuri[12] examined the problem of a hydrogenic impurity placed at the center of a $GaAs/Ga_{1-x}Al_xAs$ three-quantum-well structure which is valid for small barrier height and/or thin barriers. He found that the impurity binding energy as a function of the well width (same barrier height) exhibited a double-peak structure, with the two peaks occurring at well widths of approximately 10 and 100 Å. Lane and Green[13] have generalized Chaudhuri's calculation to a superlattice, and also calculated the energies of the low-lying excited states of a hydrogenic donor at an arbitrary position. These calculations have been extended to higher excited states by Helm *et al.*[14] Except for the calculations of Green and Bajaj, these calculations were carried out in the absence of an applied magnetic field.

Recently, Ranganathan *et al.*[15] have carried out far-infrared magnetotransmission measurements on center-well-doped Si in $GaAs/Ga_{0.7}Al_{0.3}As$ coupled double quantum wells. The measurements were made for three different samples with identical well widths (170 Å) but different narrow barrier widths (48, 18, and 9 Å). Variational calculations reported in that paper revealed that results agree with experiment for the $1s$-$2p_-$ transition energy only when a mixture of the first (symmetric) and second (asymmetric) subbands and the difference in the well and barrier masses are taken into account. Further calculations[16] revealed that the agreement with the measurements of Ref. 15 is not improved when mixing of minibands higher than the lowest two was included.

More recently, Ranganathan *et al.*[17] have extended their measurements of the ground to the first excited-state transition of the hydrogenic donor in superlattices. Two $GaAs/Ga_{0.7}Al_{0.3}As$ superlattice samples with periodicities of 89 and 49 Å were studied. In both samples, the barrier width was 9 Å while the GaAs well width for one sample was 80 Å and for the other was 40 Å; both samples were atomic planar Si-doped in the well centers. The far-infrared magnetotransmission measurements were carried out at various magnetic fields ranging from 0 to 9 T.

The object of the present paper is to study the ground and first excited states of a hydrogenic donor located at two different locations (on center and on edge of the central well) of superlattice structures with large interwell coupling. For comparison with the experiments of Ranganathan *et al.*,[17] two periodicities, 89 and 49 Å, were

0163-1829/93/48(19)/14226(6)/$06.00

studied. The number of wells plus barriers was gradually increased symmetrically with respect to the well containing the impurity. The binding energies do not change significantly for either of the structures when the number of wells plus barriers is increased from 13 to 15. Thus 15 repetitions is adequate for representation of a superlattice, and calculations were carried out for these structures in the presence of an applied magnetic field perpendicular to the interfaces. Very good agreement with the measurements was obtained.

II. METHOD OF CALCULATION

The multiple-quantum-well structure considered in this paper consists of a varying number of GaAs wells separated by thin $Ga_{1-x}Al_xAs$ barriers. A uniform magnetic field is considered parallel to the growth axis, i.e., perpendicular to the interfaces between the wells and barriers. A schematic diagram of this multiple-quantum-well structure is shown in Fig. 1.

Within the framework of the effective-mass approximation, the Hamiltonian for the donor electron placed in a finite superlattice (Fig. 1) in a magnetic field is given by

$$H=\frac{m^*}{m_e^*}\left[-\nabla^2+\gamma L_z+\frac{\gamma^2\rho^2}{4}\right]-\frac{2}{r}+V(z)\ . \tag{1}$$

Throughout the paper, atomic units for GaAs have been employed: all distances are in units of the effective Bohr radius $a_0=\hbar^2\epsilon_0/m^*e^2=98.7$ Å; all energies are in units of the effective Rydberg $R^*=m^*e^4/2\hbar^2\epsilon_0^2=5.83$ meV; and the dimensionless measure of the magnetic field is defined as $\gamma=e\hbar B/2m^*cR$, where m^* and ϵ_0 are the electronic effective mass and the static dielectric constant of GaAs, respectively. In Eq. (1), m_e^* is the effective mass of an electron, which is different in the two semiconductors, and the static dielectric constant $\epsilon_0=12.5$ is assumed to be the same in both materials. In cylindrical coordinates, the electron position is denoted by $r=\sqrt{\rho^2+(z-z_I)^2}$, where z_I is the position of the impurity atom and ρ is the distance in the x-y plane. The angular momentum operator in the z direction L_z is in units of $\hbar$. The potential $V(z)$ is modeled by a series of square-well potentials

$$V(z)=\begin{cases}0 & \text{(in the wells)}\\ V_0 & \text{(in the barriers and boundaries)}\ .\end{cases} \tag{2}$$

In the calculations outlined below, V_0 (the conduction-band offset) was taken to be 230 meV, i.e., 60% of the energy gap difference between GaAs and $Ga_{0.7}Al_{0.3}As$.

A variational approach is used to calculate the eigenvalues of the Hamiltonian. Including the mixing of the miniband states, the trial wave function is chosen to be

$$\Psi(\rho,z,\phi)=G(\rho,z-z_I,\phi)\sum_{j=1}^{N}a_jf_j(z)\ , \tag{3}$$

where the summation is taken over the miniband states of a free electron in the one-dimensional multiple quantum wells with the potential $V(z)$. The coefficients a_j are variational parameters subject to the normalization constraint

$$\sum_{j=1}^{N}|a_j|^2=1\ , \tag{4}$$

and N is chosen such that the inclusion of miniband states higher than N does not change the results more than 0.002 effective Ry (N is 4 in our calculations). The function $f_j(z)$ is

$$f_j(z)=\alpha_{ji}e^{K_{ji}z}+\beta_{ji}e^{-K_{ji}z}\ , \tag{5}$$

where the indices j and i denote the jth subband and the ith region (see Fig. 1), respectively. By taking $f_j(z)$ and $(1/m_e^*)df_j/dz$ to be continuous across the interfaces, K_{ji} and other coefficients are determined following the work of Zang and Rustigi;[18] this is briefly outlined in the Appendix.

The cylindrical symmetry of the Hamiltonian ensures that the ϕ dependence of the wave function has the form $e^{im\phi}$, where m is the quantum number associated with the angular momentum in the z direction. The function $G(\rho,z-z_I,\phi)$ is

$$G(\rho,z-z_I,\phi)=\rho^{|m|}e^{im\phi}\sum_{ij}A_{ij}G_{ij}(\rho,z-z_I)\ . \tag{6}$$

The Gaussian basis functions $G_{ij}(\rho,z-z_I)$ are given by

$$G_{ij}(\rho,z-z_I)=e^{-\alpha_i(z-z_I)^2}e^{-(\alpha_j+\beta)\rho^2}\ . \tag{7}$$

In Eqs. (6) and (7), β and A_{ij} are variational parameters; the set of parameters α_i is taken from Table I of Ref. 10. The number of basis functions is restricted by requiring $A_{ij}=0$ for $|i-j|>1$, which gives 13 and 10 basis functions, respectively, for the ground and first excited states. The eigenvalues $E_1(m=0)$ and $E_2(m=-1)$ are determined by numerically minimizing

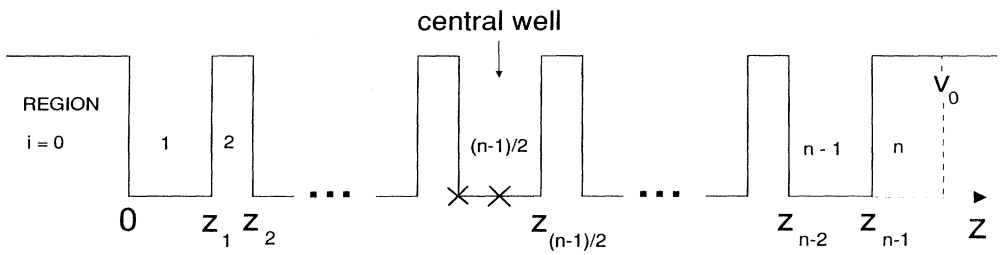

FIG. 1. Schematic illustration of the multiple-quantum-well structure. The ×'s indicate two positions of the donor ion considered; i.e., on center and on edge of the central well.

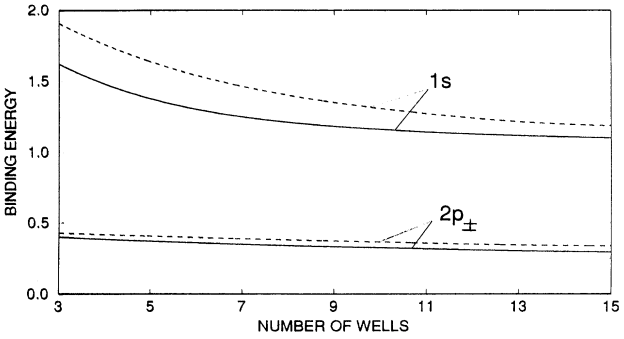

FIG. 2. Binding energies (in units of effective Rydberg) of the $1s$ and $2p_{\pm}$ states as functions of the number of wells for the on-center location of the impurity in the central well at zero magnetic field. The solid and dashed curves display the results for the two different periodicities: the 80-Å well, 90-Å barrier, and the 40-Å well, 9-Å barrier, respectively.

$\langle \Psi|H|\Psi\rangle / \langle \Psi|\Psi\rangle$.

The binding energies for the ground (E_{1s}) and first excited (E_{2p_-}) states are

$$E_{1s}=E_0+\gamma-E_1, \quad E_{2p_-}=E_0+\gamma-E_2 , \tag{8}$$

where E_0 is the lowest energy of a free electron in the potential $V(z)$ given by Eq. (2) (the energy of the lowest miniband) and γ is the energy of the lowest Landau level.

III. RESULTS AND DISCUSSION

The binding energies of the ground ($1s$) and first excited ($2p_{\pm}$) states at zero magnetic field are plotted in Figs. 2 and 3 as functions of the number (3,5,7, . . . , 15) of wells for two different locations of the impurity within the central well, on center and on edge, respectively. Two different periodicities are considered: the 80-Å well, 9-Å barrier (solid curves) and the 40-Å well, 9-Å barrier (dashed curves). The results show that in all cases for the same periodicity when the number of wells is increased, the electron is less confined, so that its binding energy is reduced. After about 13 wells the curves become almost horizontal, i.e., the binding energy does not change as the number of wells is further increased because the two outer boundaries of the multiple-quantum-well structure are far enough from the hydrogenic impurity that their effect on the binding electron becomes insignificant. This asymptotic or superlattice behavior is obtained at a smaller number of wells in the 80-Å well, 9-Å barrier case than for the 40-Å well, 9-Å barrier case due to the smaller well size of the latter case. For the 80-Å well, 9-Å barrier structure, as the number of periods is increased from 13 to 15, the binding energies for both the $1s$ and $2p$ states change only by $0.01R^*$, while for the 40-Å well, 9-Å barrier superlattice the energies change by $0.04R^*$ and $0.01R^*$, respectively. This asymptotic behavior can be understood more clearly by examining Figs. 4–7, which show the probability density of the donor electron as a function of z for the on-center location of the impurity in the central well for structures having two different repetitions, 5 and 15, and with two periodicities, 89 and 49 Å in zero magnetic field. This probability density is obtained by integrating the square of the wave function [Eq. (5)] over ρ and ϕ. In Figs. 4 and 6, the five-quantum-well model, the electron still has significant probability at the two outer boundaries, especially for the 49-Å periodicity

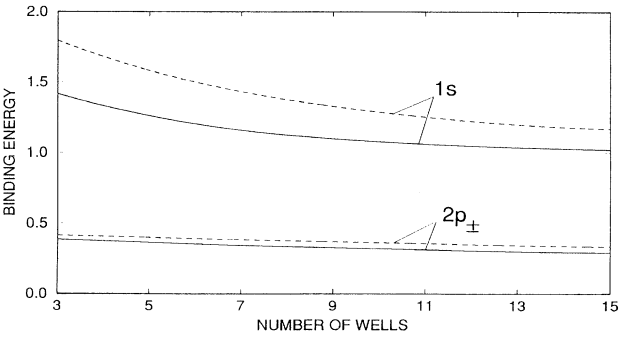

FIG. 3. Same as Fig. 2, but for the on-edge location of the impurity in the central well.

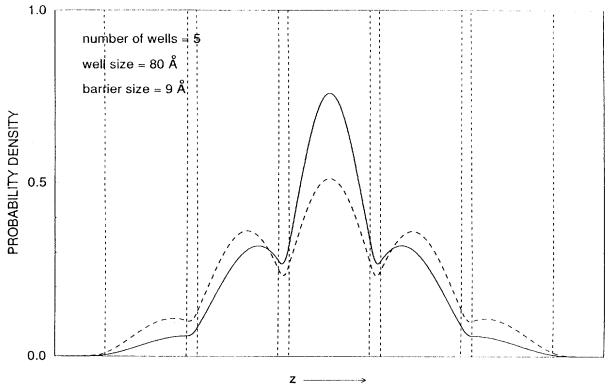

FIG. 4. Probability density of the donor electron in the $1s$ (solid curve) and $2p_{\pm}$ (dashed curve) states as functions of z for the on-center location of the impurity in the central well of a five quantum-well structure, with 80-Å wells and 9-Å barriers in zero magnetic field. The vertical dashed lines indicate the interfaces of the two semiconductors, the boundaries of the barriers.

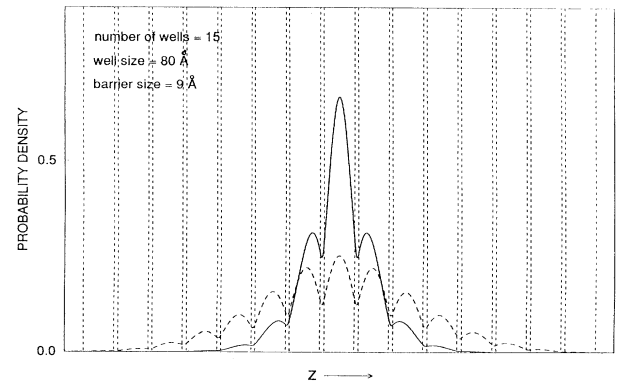

FIG. 5. Same as Fig. 4, but for a 15 quantum-well structure.

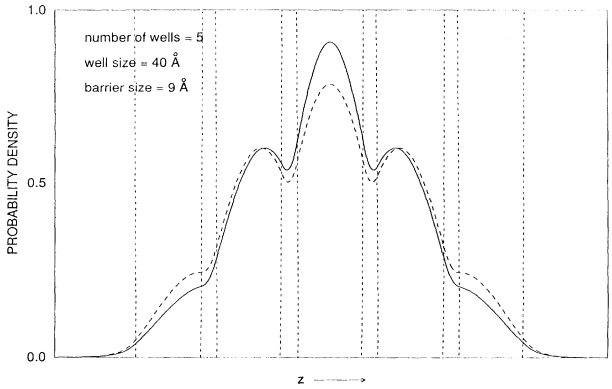

FIG. 6. Same as Fig. 4, but for the 40-Å well, 9-Å barrier structure.

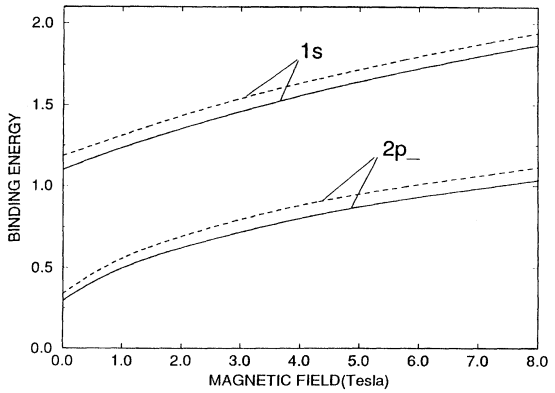

FIG. 8. Binding energies (in units of effective Rydberg) of the $1s$ and $2p_-$ states as functions of the applied magnetic field oriented normal to the wells for the on-center location of the impurity in the central well. The solid and dashed curves display the results for the two different superlattices (15 wells) with periodicities of the 80-Å well, 9-Å barrier and the 40-Å well, 9-Å barrier, respectively.

case; this emphasizes that a five-well model is not an adequate representation of a superlattice for such narrow wells and barriers. Figures 5 and 7, the 15-quantum-well model, show that the electron spreads into many wells beyond that containing the impurity, but the electron probability is almost unnoticeable at the two outer boundaries; the asymptotic or superlattice behavior is obtained a about 13 and 15 wells for the 89- and 49-Å periodicity cases, respectively. Figures 4–7 also show that the asymptotic behavior is obtained at a smaller number of wells for the $1s$ state than for the $2p$ state due to the larger effective radius of the latter.

Figures 8 and 9 depict the binding energies of the ground ($1s$) and first excited ($2p_-$) states as functions of the applied magnetic field for two locations of the impurity, on center and on edge, within the central well of the superlattice structure, respectively. Each of the two considered superlattices consists of 15 quantum wells with the periodicity of either 89 Å (solid curves) or 49 Å (dashed curves). All the curves show that the binding energy increases as the magnetic field increases because of the larger increase of the lowest Landau level ($\gamma \propto B$) compared with those of the eigenvalues E_1 ($m=0$) and E_2 ($m=-1$) in Eqs. (8). The applied magnetic field also confines the electron more around the impurity; this additional confinement of the electron reduces the number of wells at which the asymptotic behavior (superlattice) is obtained.

In general, for the same number of wells, the binding energy in the 40-Å well, 9-Å barrier case is always larger than the corresponding one in the 80-Å well, 9-Å barrier case because of larger extent or weaker confinement of the electron in the z direction in the latter case (larger well size). For the same periodicity and same number of wells, the binding energy for the on-center impurity case is always larger than that for the on-edge impurity case because in the latter case the barrier next to the impurity pushes the electron away so that it becomes less confined around the impurity.

The effects of the mixing of the miniband states, as explained in Ref. 16, result from an interplay between two opposing effects. One effect is that, due to the mixing of different miniband states, the electron is more confined in the z direction, and this increases the negative Coulomb

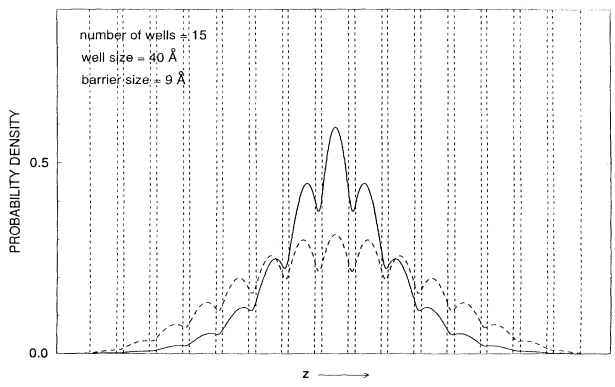

FIG. 7. Same as Fig. 6, but for a 15 quantum-well structure.

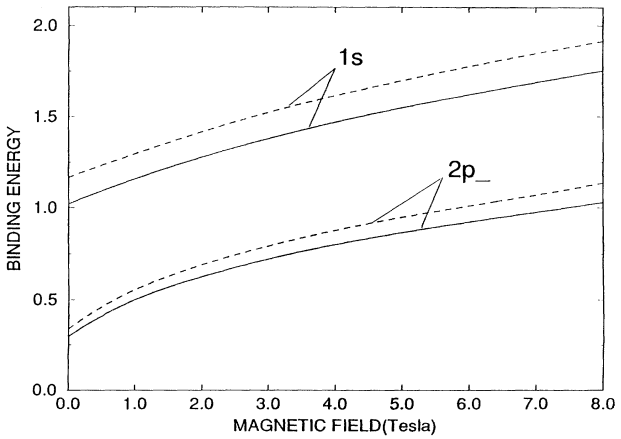

FIG. 9. Same as Fig. 8, but for the on-edge location of the impurity in the central well.

potential energy, thus raising the binding energy. The second effect is that the inclusion of the higher miniband states raises the kinetic energy, thus reducing the binding energy. Although the calculations in this paper are carried out including mixing of the miniband states associated with the four lowest subbands of the isolated wells, comparison with the nonmixing calculations (only the single lowest miniband state was considered) does not show significant numerical differences, at most the difference is about $0.01R^*$. Mixing of the minibands is more pronounced in the 80-Å well, 9-Å barrier case than in the 40-Å well, 9-Å barrier case due to the larger energy difference between the minibands in the latter structure. The mixing also depends on the number of wells considered; in general, as the number of wells is increased, the energy gap between the minibands is decreased so that mixing is increased.

Figures 10 and 11 show a comparison of our calculations with the measurements of Ref. 18 for the donor transition energy of $1s$-$2p_-$ states vs magnetic field. Since the $1s$-$2p_-$ transition energy was difficult to determine accurately in the transmission experiment, it was obtained by taking the difference between the measured $1s$-$2p_+$ transition energy and the corresponding experimental value of 2γ (the cyclotron resonance energy which is the energy difference between the $2p_-$ and $2p_+$ states). The agreement is very good. It is clear from the small differences in the transition frequencies between the well-center and well-edge impurities that a uniform distribution of impurities within the well for these samples would not contribute significantly to inhomogeneous broadening of absorption lines for these superlattice structures. Thus the large inhomogeneously broadened linewidths reported for uniformly doped superlattices[19] cannot be due to distribution within the wells (or the narrow barriers). It is most likely that such inhomogeneous broadening results from the finite superlattice and contributions from impurities in wells that are close to the "top" and "bottom" of the entire structure.

In conclusion, our results show that the binding energy of a hydrogenic impurity in the multiple-quantum-well structure depends strongly upon the number and size of the periodicities, the location of the impurity, and the applied magnetic field. The dependence of the binding energy upon the number of wells decreases as the number of wells is increased until the asymptotic behavior is approached, and then the multiple-quantum-well structure can be considered as a superlattice structure; for shallow donors in $GaAs/Ga_{0.7}Al_{0.3}As$ structures, this number is about 15.

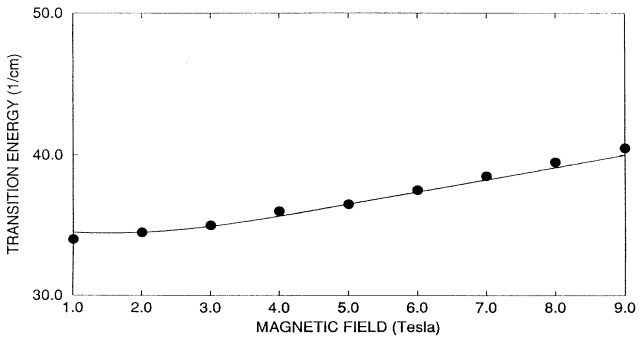

FIG. 10. The measure (Ref. 17) (solid circles) and calculated (lines) hydrogenic donor transition energy between the ground ($1s$) and first excited ($2p_-$) states vs magnetic field for the on-center location of the impurity in the 80-Å well, 9-Å barrier superlattice.

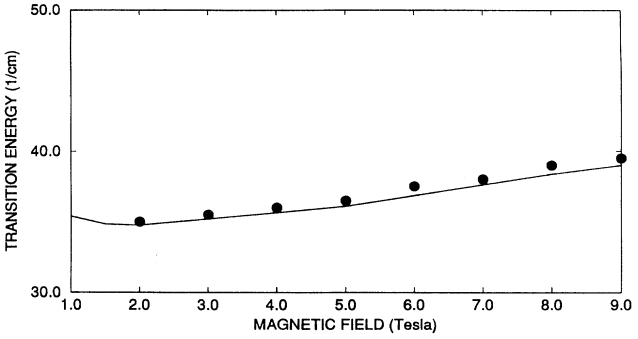

FIG. 11. Same as Fig. 10, but for the 40-Å well, 9-Å barrier superlattice.

APPENDIX

For the multiple-quantum-well structure given in Fig. 1, the Schrödinger equation for a free electron in the ith region can be written in atomic units of GaAs as

$$\frac{d^2F_i}{dz^2}+K_i^2F_i=0\ , \tag{A1}$$

where F_i is the wave function of the electron in the z direction,

$$F_i=\alpha_i e^{K_i z}+\beta_i e^{-K_i z}\ , \tag{A2}$$

and the wave number K_i is given by

$$K_i=\left[\frac{m_i^*}{m^*}(V_i-E)\right]^{1/2}\ , \tag{A3}$$

where m^* and m_i^* are the effective mass of the electron in GaAs and in the ith region, respectively.

The continuity conditions of F_i and $(1/m_i^*)dF_i/dz$ across the interfaces z_i give

$$\alpha_i e^{K_i z_i}+\beta_i e^{-K_i z_i}=\alpha_{i+1}e^{K_{i+1}z_i}+\beta_{i+1}e^{-K_{i+1}z_i} \tag{A4}$$

and

$$\frac{K_i\alpha_i}{m_i^*}e^{K_i z_i}-\frac{K_i\beta_i}{m_i^*}e^{-K_i z_i} =\frac{K_{i+1}\alpha_{i+1}}{m_{i+1}^*}e^{K_{i+1}z_i}=\frac{K_{i+1}\beta_{i+1}}{m_{i+1}^*}e^{-K_{i+1}z_i}\ . \tag{A5}$$

Equations (A4) and (A5) can be written in matrix form as

$$M_i(z_i)\begin{bmatrix}\alpha_i\\ \beta_i\end{bmatrix}=M_{i+1}(z_i)\begin{bmatrix}\alpha_{i+1}\\ \beta_{i+1}\end{bmatrix}\ , \tag{A6}$$

where

$$M_i(z)=\begin{bmatrix} e^{K_i z} & e^{-K_i z} \\ \dfrac{K_i}{m_i^*}e^{K_i z} & -\dfrac{K_i}{m_i^*}e^{-K_i z} \end{bmatrix} . \tag{A7}$$

In matrix form, the boundary conditions across all the interfaces of the multiple quantum wells give

$$\begin{aligned} &M_0(0)\begin{bmatrix}\alpha_0\\ \beta_0\end{bmatrix}=M_1(0)\begin{bmatrix}\alpha_1\\ \beta_1\end{bmatrix} , \\ &\quad\vdots \\ &M_i(z_i)\begin{bmatrix}\alpha_i\\ \beta_i\end{bmatrix}=M_{i+1}(z_i)\begin{bmatrix}\alpha_{i+1}\\ \beta_{i+1}\end{bmatrix} , \\ &\quad\vdots \\ &M_{n-1}(z_{n-1})\begin{bmatrix}\alpha_{n-1}\\ \beta_{n-1}\end{bmatrix}=M_n(z_{n-1})\begin{bmatrix}\alpha_n\\ \beta_n\end{bmatrix} . \end{aligned} \tag{A8}$$

The multiplication of every equation in (A8) by the inverse matrix of the corresponding one on the left-hand side gives

$$\begin{aligned} &\begin{bmatrix}\alpha_0\\ \beta_0\end{bmatrix}=M_0^{-1}(0)M_1(0)\begin{bmatrix}\alpha_1\\ \beta_1\end{bmatrix} , \\ &\quad\vdots \\ &\begin{bmatrix}\alpha_i\\ \beta_i\end{bmatrix}=M_i^{-1}(z_i)M_{i+1}(z_i)\begin{bmatrix}\alpha_{i+1}\\ \beta_{i+1}\end{bmatrix} , \\ &\quad\vdots \\ &\begin{bmatrix}\alpha_{n-1}\\ \beta_{n-1}\end{bmatrix}=M_{n-1}^{-1}(z_{n-1})M_n(z_{n-1})\begin{bmatrix}\alpha_n\\ \beta_n\end{bmatrix} . \end{aligned} \tag{A9}$$

The combination of Eqs. (A9) together with the condition $\beta_0=\alpha_n=0$ for the bound state of the electron gives

$$\begin{bmatrix}\alpha_0\\ 0\end{bmatrix}=T\begin{bmatrix}0\\ \beta_n\end{bmatrix} , \tag{A10}$$

where

$$\begin{aligned} T=&M_0^{-1}(0)M_1(0)M_1^{-1}(z_1)M_2(z_1)\cdots \\ &\times M_{i-1}^{-1}(z_{i-1})M_i(z_{i-1})M_i^{-1}(z_i)M_{i+1}(z_i)\cdots \\ &\times M_{n-1}^{-1}(z_{n-1})M_n(z_{n-1})=\begin{bmatrix}T_{11} & T_{12}\\ T_{21} & T_{22}\end{bmatrix} , \end{aligned} \tag{A11}$$

and

$$T_{22}=0 . \tag{A12}$$

The energy eigenvalues can be found from Eq. (A12). By setting $\alpha_0=1$ in Eq. (A10) the coefficient β_n is given by

$$\begin{bmatrix}0\\ \beta_n\end{bmatrix}=T^{-1}\begin{bmatrix}1\\ 0\end{bmatrix} , \tag{A13}$$

and all other coefficients can be obtained by using Eqs. (A9).

[1]K. F. Brennan and C. J. Summers, J. Appl. Phys. **61**, 614 (1987).
[2]F. Capasso, K. Mohamed, and A. Y. Cho, IEEE J. Quantum Electron. **22**, 1853 (1986).
[3]T. C. L. G. Sollner, E. R. Brown, and H. Q. Lelincoln, Lab. J. **1**, 89 (1988).
[4]R. Tsu and L. Esaki, Appl. Phys. Lett. **22**, 562 (1973).
[5]F. Capasso and R. A. Kiehl, J. Appl. Phys. **58**, 1366 (1985).
[6]F. Capasso, S. Sen, A. Y. Cho, and D. Sivco, IEEE Electron Device Lett. **8**, 297 (1987).
[7]S. Sen, F. Capasso, A. Y. Cho, and D. Siveo, IEEE Trans. Electron Device **34**, 2185 (1987).
[8]G. Bastard, Phys. Rev. B **24**, 4714 (1981).
[9]C. Mailhiot, Y. C. Chang, and T. C. McGill, Phys. Rev. B **26**, 4449 (1982).
[10]R. L. Greene and K. K. Bajaj, Phys. Rev. **31**, 913 (1985).
[11]N. C. Jarosik, B. D. McCombe, B. V. Shannabrook, J. Comas, J. Ralston, and G. Wicks, Phys. Rev. Lett. **54**, 1283 (1985).
[12]S. Chaudhuri, Phys. Rev. B **28**, 4480 (1983).
[13]P. Lane and R. L. Green, Phys. Rev. B **33**, 5871 (1986).
[14]M. Helm, F. M. Peeters, F. Derosa, E. Colas, J. P. Harbison, and L. T. Florez, Phys. Rev. B **43**, 13 983 (1991).
[15]R. Ranganathan, B. D. McCombe, N. Nguyen, Y. Zhang, M. L. Rustgi, and W. J. Schaff, Phys. Rev. B **44**, 1423 (1991).
[16]N. Nguyen, R. Ranganathan, B. D. McCombe, and M. L. Rustgi, Phys. Rev. B **44**, 3344 (1991); **45**, 11 166 (1992).
[17]R. Ranganathan, B. D. McCombe, N. Nguyen, and M. L. Rustgi (unpublished).
[18]J. X. Zang and M. L. Rustgi, Infrared Phys. **31**, 621 (1991); **33**, 175 (1992).
[19]T. Duffield, R. Bhat, M. Koza, M. C. Tarmago, T. P. Harbison, F. deRosa, D. M. Hwang, P. Grabbe, and S. J. Allen, Jr., Solid State Commun. **60**, 557 (1960).